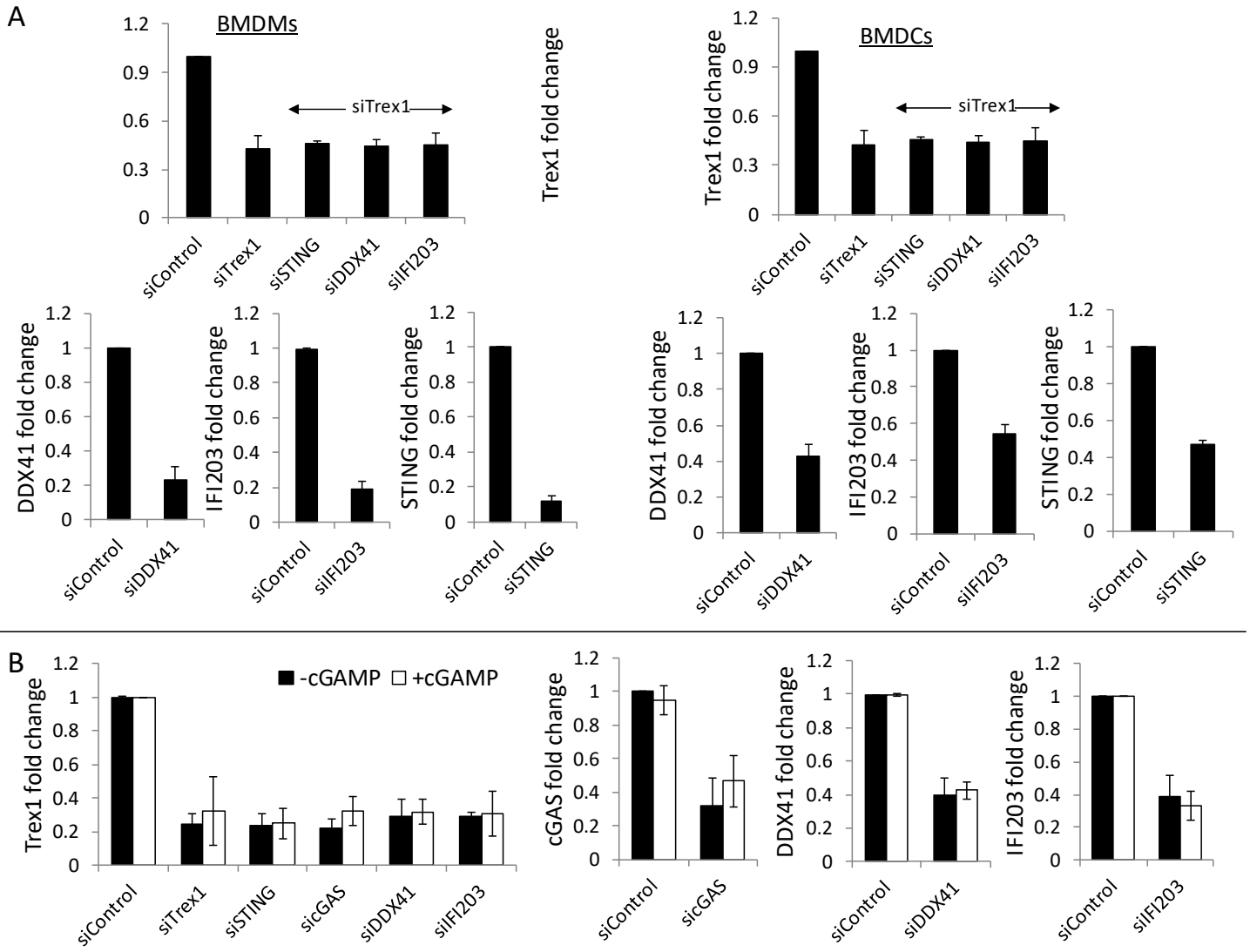

Fig. S1. Knockdown verification. Related to Fig. 1. A) Knockdown of genes in Fig. 1A. The knockdown of the three target genes (DDX41, IFI203 an STING) were all done in the presence of Trex1 knockdown, as indicated in the Fig. 1 legend. B) Knockdown of genes in Fig. 1C. See Fig. 1 legend for details.

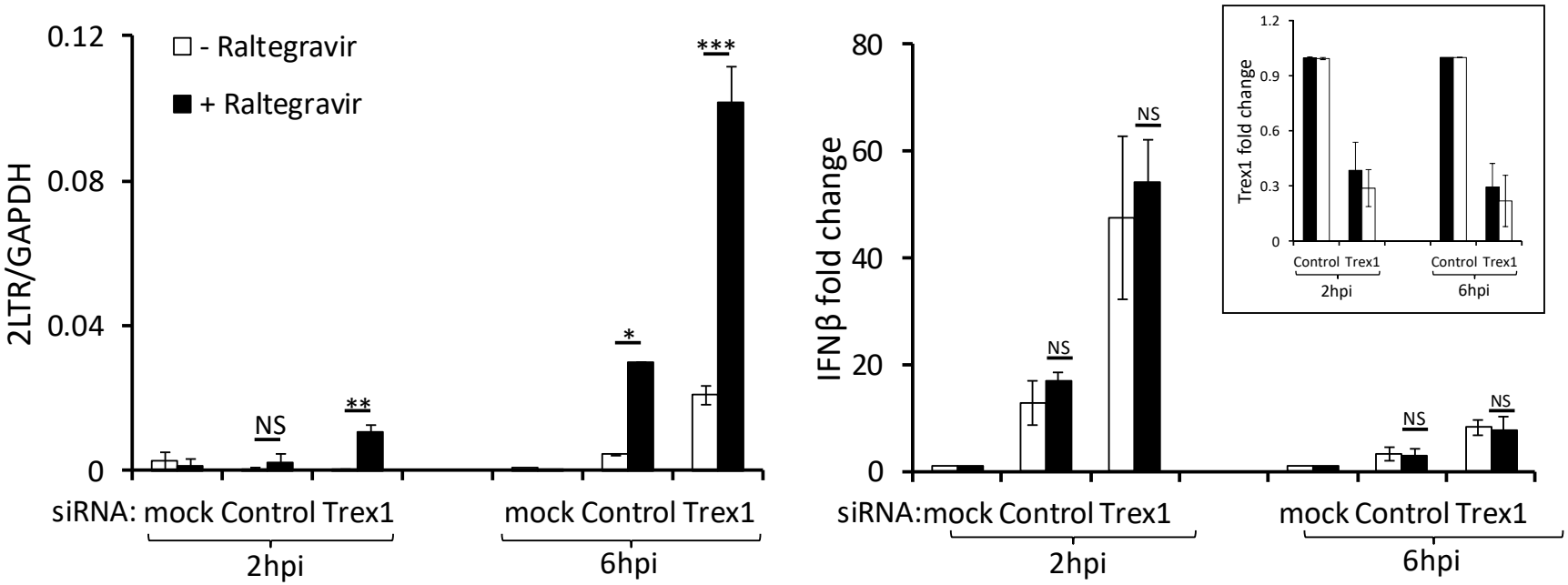

Fig. S2. DDX41 senses DNA in the cytoplasm via its DEAD domain. Related to Fig. 2. A) Increasing nuclear dsDNA by inhibiting proviral DNA integration has no effect on DDX41-mediated sensing. NR9456 cells were pretreated with raltegravir (200nM) and then infected with MLV (MOI=2) in the presence of drug. DNA and RNA were isolated from infected cells 2 hpi and analyzed for unintegrated viral DNA (2LTR) or IFNβ RNA levels. Values are shown as mean ± STDs of three experiments. P values were determined by an unpaired T-test. (*, p≤ 0.05; **, p≤ 0.01; ***, p≤ 0.001). Inset shows levels of Trex1 RNA knockdown.

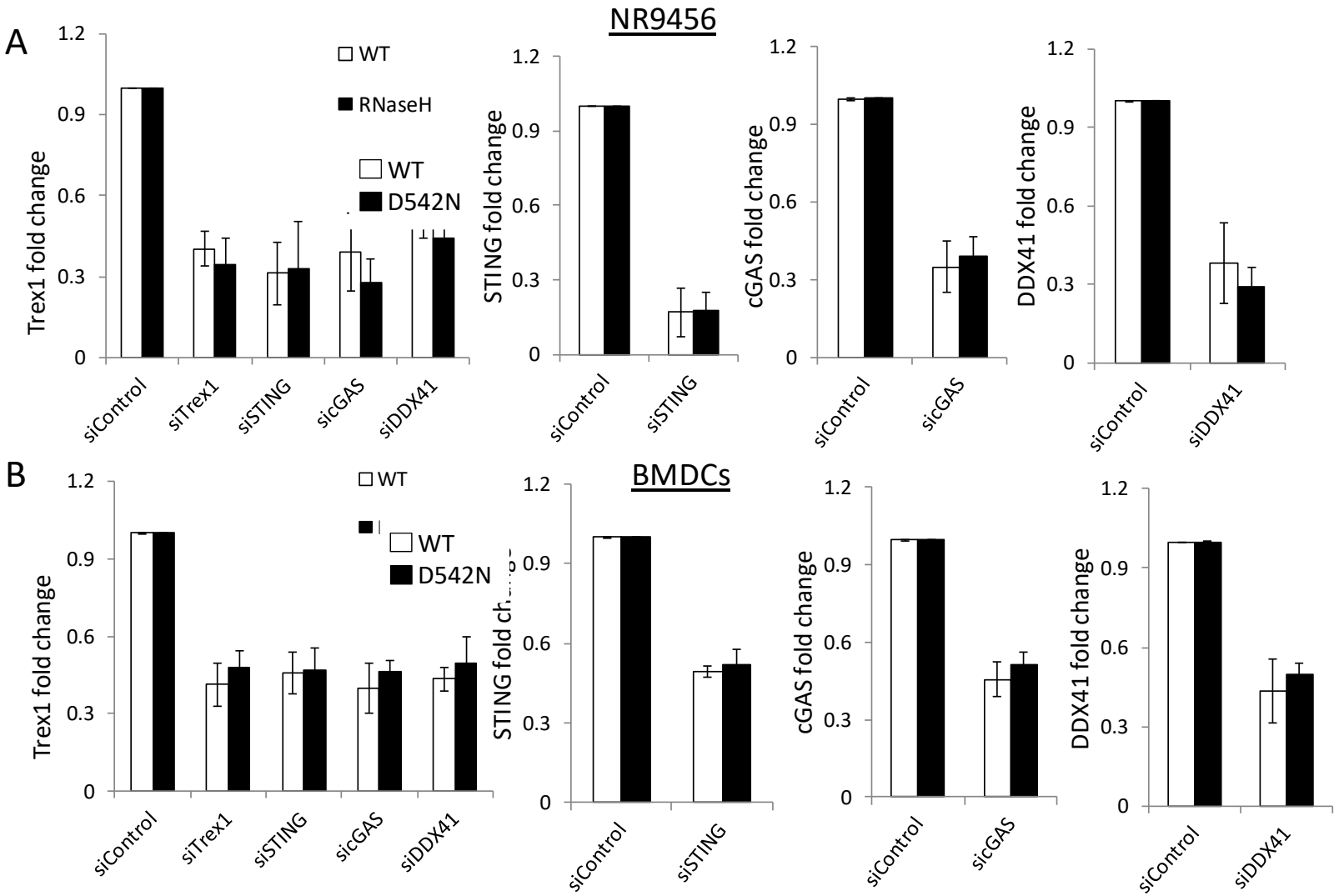

Fig. S3. Knockdown verification. Related to Fig. 4. A) Knockdown of genes in Fig. 4C. See Fig. 4 legend for details.

A

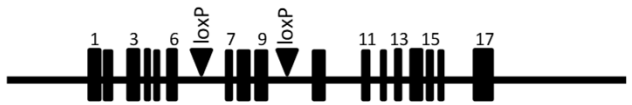

B

	BMDMs			BMDCs		
Mouse Strain	**STING**	**DDX41**	**cGAS**	**STING**	**DDX41**	**cGAS**
C57BL/6	1.243 ± .435	0.731 ± .363	0.654 ± .114	0.666 ± .476	0.530 ± .209	0.170± .02
STING$^{gt/gt}$	0.006 ± .004	0.495 ± .316	0.368 ± .132	0.014 ± .021	0.335 ± .164	0.214 ± .128
cGAS KO	1.294 ± .192	0.670 ± .260	0.001 ± .001	0.65 ± .505	1.10 ± .139*	0.003 ± .003
CD11cCre DDX41$^{fl/fl}$	1.378 ± .778	0.537 ± .267	0.834 ± .661	1.00±.370	0	0.278±.075
LyCre DDX41$^{fl/fl}$	1.237 ± .486	0.003 ± .005	1.407 ± .744	0.89 ± .332	0.469±.172	0.29± .11

C

	IFNβ/actin (x10^{-3})	
Mouse	BMDM	BMDC
C57BL/6	0.017 ± 0.002	1.1 ± 0.7
STING$^{gt/gt}$	0.015 ± 0.021	ND
cGAS KO	0.016 ± 0.003	0.8 ± 0. 1
LyCre DDX41$^{fl/fl}$	0.022 ± 0.003	ND
CD11cre DDX41$^{fl/fl}$	ND	0. 9 ± 0. 6

D

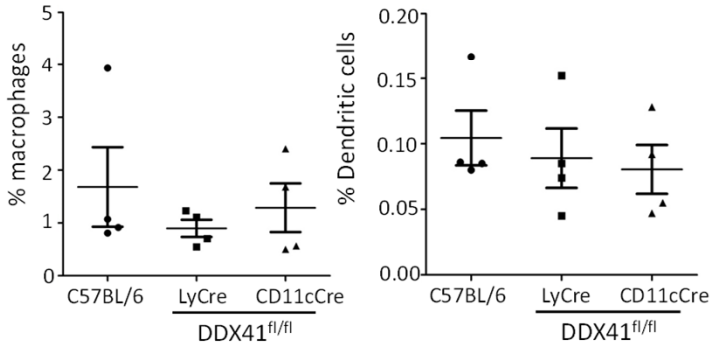

E

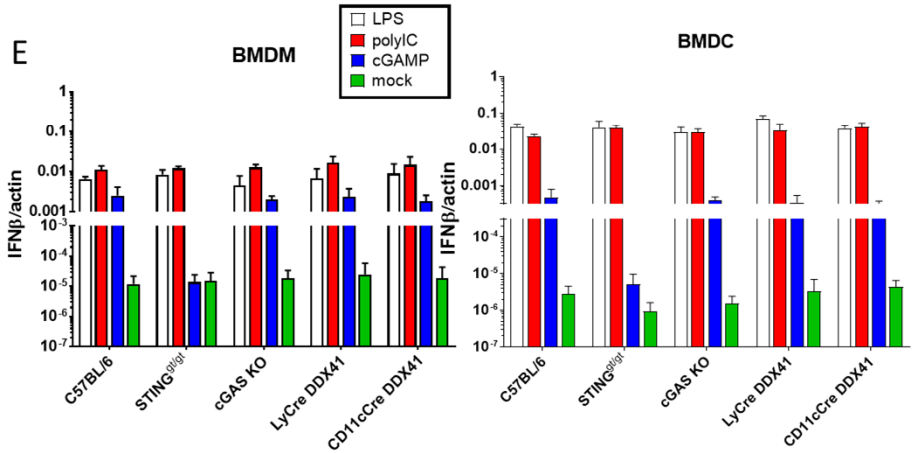

Fig. S4. Characterization of DDX41 KO mice. Related to Fig. 5 and 6. A) Map of the DDX41 locus and inserted lox P sites. Expression of Cre recombinase results in the deletion of exons 7 - 9. B) Quantification of DDX41, cGAS and STING protein in various knockout mouse cells. Shown is the mean +/- STD for 3 independent western blots of cells from 3 different mice of each strain. *, $p \leq 0.05$ compared to BL/6, STING$^{gt/gt}$ and CD11cCreDDX41 (unpaired T-Test). C) Basal IFNβ RNA levels in DDX41 KO BMDMs and BMDCs. RNA was isolated from BMDMS of 3 mice and BMDCs of 2 mice each of the indicated genotypes and qPCR was performed for IFNβ levels, using a standard curve to measure relative levels. Shown is the mean +/- STD. Abbreviations: ND, not done. D) PBMCs from 4 mice of each genotype were stained with conjugated anti-CD11c (DCs) or anti-F4/80 (macrophages) antibodies and analyzed by FACS. E) Treatment of DDX41 KO BMDMs and BMDCs with different ligands. BMDMs and BMDCs from the cGAS, LyCre DDX41 and CD11cCre-DDX41 KO and STING$^{gt/gt}$ mice were treated with the indicated ligands, as described in Supplemental Experimental Procedures. RNA was isolated after 6 hr of treatment for all ligands and subjected to RT-qPCR. Shown is the average of 2 experiments (triplicate technical replicates) with cells isolated from different mice.

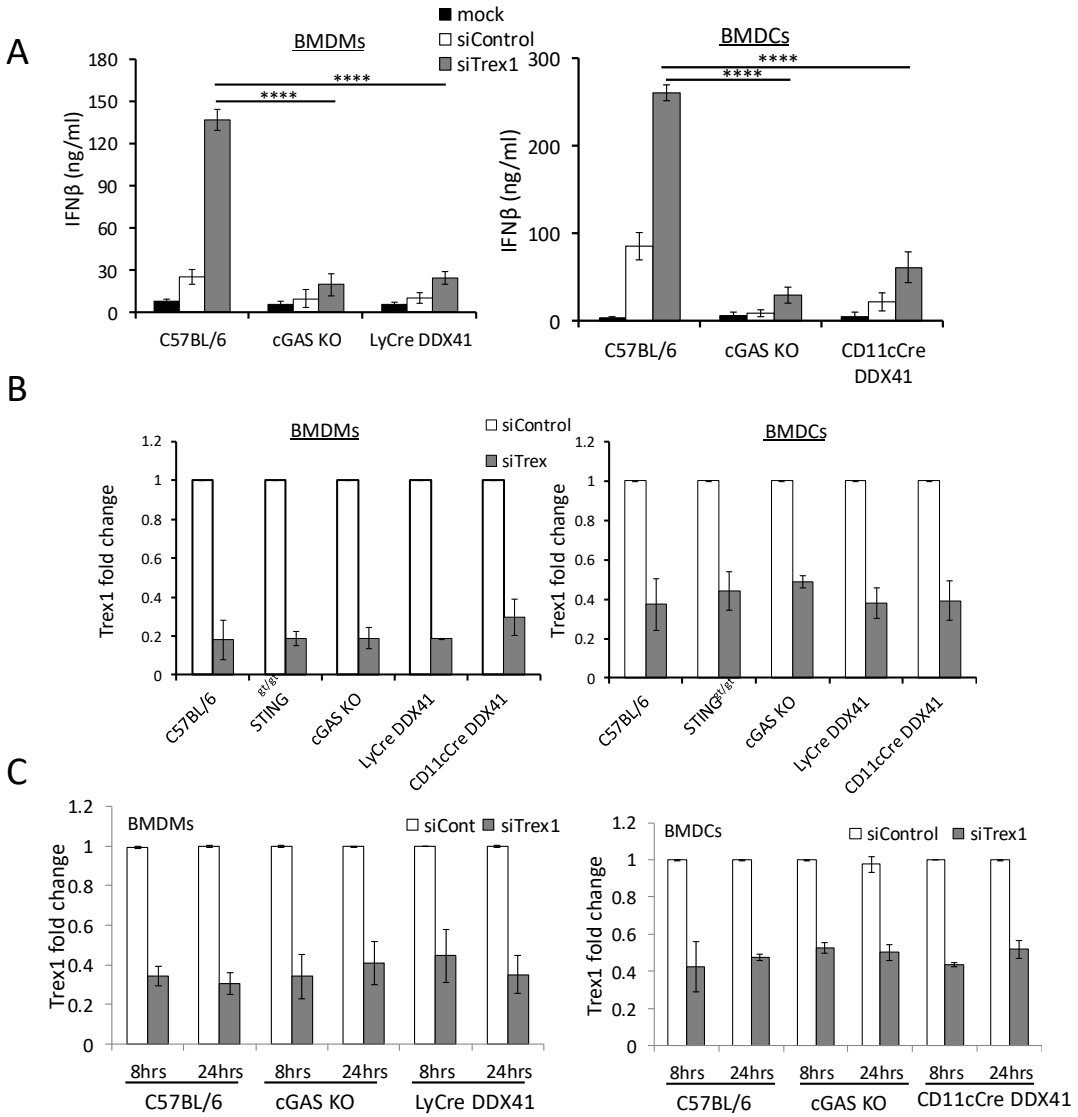

Fig. S5. Loss of DDX41 decreases the IFN response to MLV and HIV infection. Related to Fig. 6. A) BMDMs and BMDCs from C57, cGAS, LyCre-DDX41 and CD11cCre-DDX41 were treated siCont or siTrex and then infected with MLV^{glycoGag}. Four hrs later supernatants were used to perform an ELISA for IFNβ levels. Shown are the average of 3 independent experiments. ****, p≤ 0.0001 (unpaired T-test). B) Verification of Trex1 knockdown in BMDCs and BMDMs in Fig. 6A. C) Verification of the knockdowns in BMDMs and BMDCs in Fig. 6B.

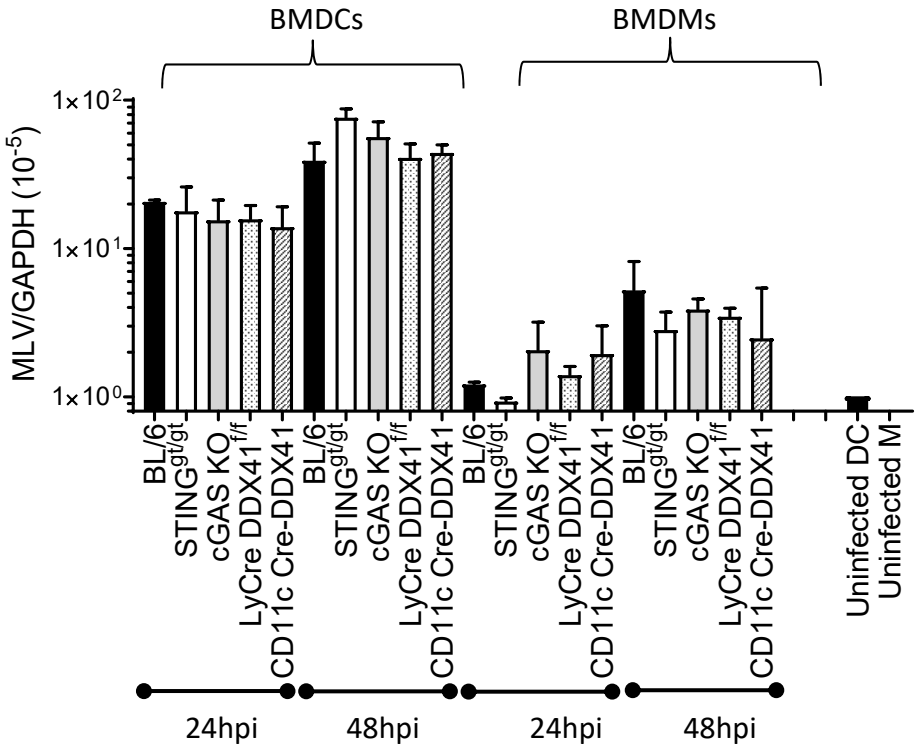

Fig. S6. BMDCs are more infected by MLV than BMMS. Related to Fig. 6. BMDMs and BMDCs from mice of the indicated genotypes were infected with MLV and at 24 and 48 hr pi infection, DNA was isolated from cells and subjected to qPCR, using one primer to mouse genomic DNA and the other to the viral long terminal repeat. Values are shown and mean ± SEM of 2 experiments done for each cell type. highlighted boxes refer to homozygous and white boxes to heterozygous DDX41 tissue-specific knockouts, gray boxes refer to WT mice.

A

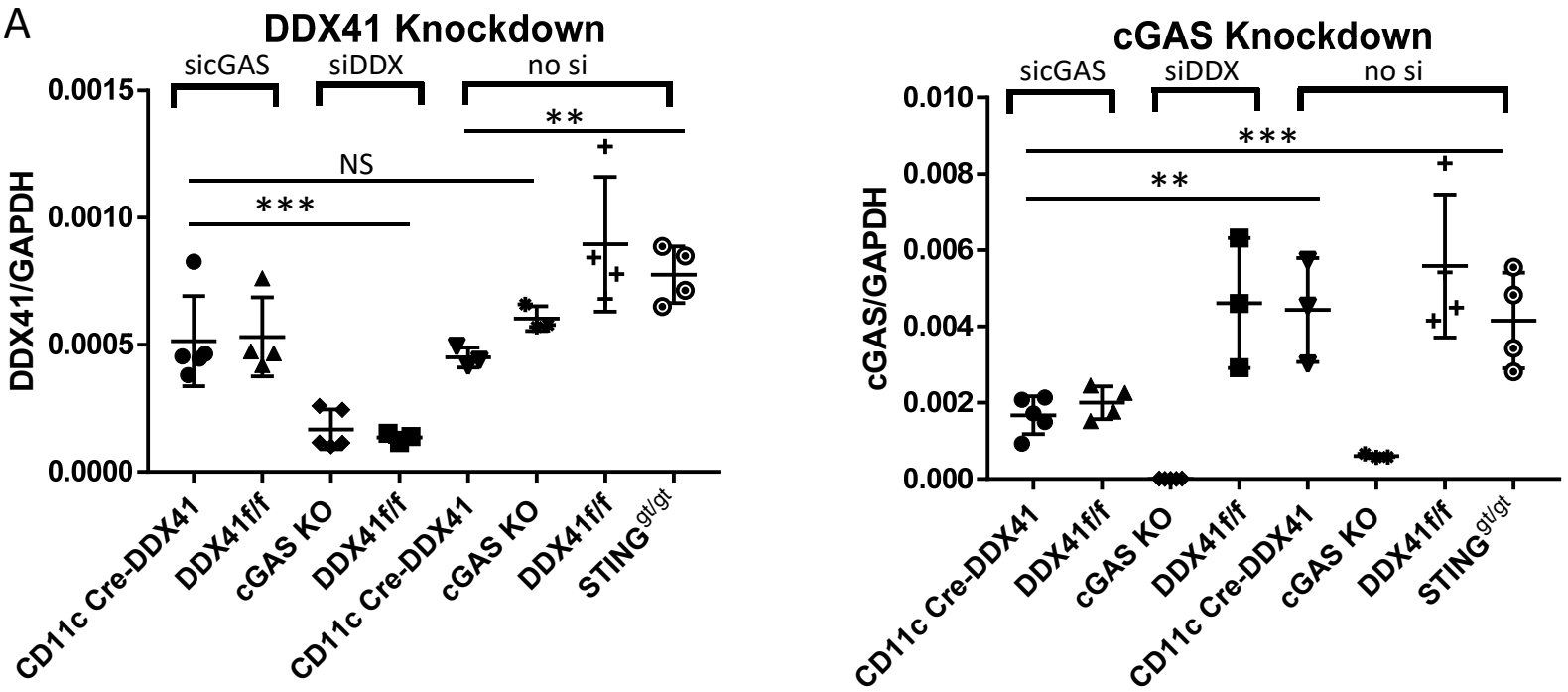

Parental genotypes	Cre+,DDX41+	Cre-,DDX41+	Cre+,DDX41-	Cre-,DDX41-
Cre+,DDX41+	Cre+/+, DDX41+/+	Cre+/-, DDX41+/+	Cre+/+, DDX41+/-	Cre+/-, DDX41+/-
Cre-,DDX41+	Cre+/-, DDX41+/+	Cre-/-, DDX41+/+	Cre+/-, DDX41+/-	Cre-/-, DDX41+/-
Cre+,DDX41-	Cre+/+, DDX41+/-	Cre+/-, DDX41+/-	Cre+/+, DDX41-/-	Cre+/-, DDX41-/-
Cre-,DDX41-	Cre+/-, DDX41+/-	Cre-/-, DDX41+/-	Cre+/-, DDX41-/-	Cre-/-, DDX41-/-

Fig. S7. *In vivo* control of retrovirus infection requires both cGAS and DDX41. Related to Fig. 7. A) Knockdown verification of the in vivo siRNA experiment presented in Fig. 7A. B) Genotypes of the mice tested for MLV infection in Fig. 7B. Parental mice were Cre+/-, DX41+/-. Cre refers to either LyCre or CD11cCre, as indicated in the text. Yellow highlighted boxes refer to homozygous and white boxes to heterozygous DDX41 tissue-specific knockouts, gray boxes refer to WT mice.